



HAL
open science

Dynamic modeling highlights the major impact of droplet coalescence on the in vitro digestion kinetics of a whey protein stabilized submicron emulsion

Thuy Minh Giang, Steven Le Feunteun, Sebastien Gaucel, Pierre Brestaz, Marc Anton, Anne Meynier, Ioan-Cristian Trelea

► To cite this version:

Thuy Minh Giang, Steven Le Feunteun, Sebastien Gaucel, Pierre Brestaz, Marc Anton, et al.. Dynamic modeling highlights the major impact of droplet coalescence on the in vitro digestion kinetics of a whey protein stabilized submicron emulsion. *Food Hydrocolloids*, 2015, 43, pp.66-72. 10.1016/j.foodhyd.2014.04.037 . hal-01195524

HAL Id: hal-01195524

<https://hal.science/hal-01195524>

Submitted on 11 Jul 2017

HAL is a multi-disciplinary open access archive for the deposit and dissemination of scientific research documents, whether they are published or not. The documents may come from teaching and research institutions in France or abroad, or from public or private research centers.

L'archive ouverte pluridisciplinaire **HAL**, est destinée au dépôt et à la diffusion de documents scientifiques de niveau recherche, publiés ou non, émanant des établissements d'enseignement et de recherche français ou étrangers, des laboratoires publics ou privés.

1 **Dynamic modeling highlights the major impact of droplet coalescence on**
2 **the *in vitro* digestion kinetics of a whey protein stabilized submicron**
3 **emulsion**

4
5 T.M. Giang^{1,2}, S. Le Feunteun^{1,2,*}, S. Gaucel^{1,2}, P. Brestaz³, M. Anton³, A. Meynier³, and I.C.
6 Trelea^{1,2}

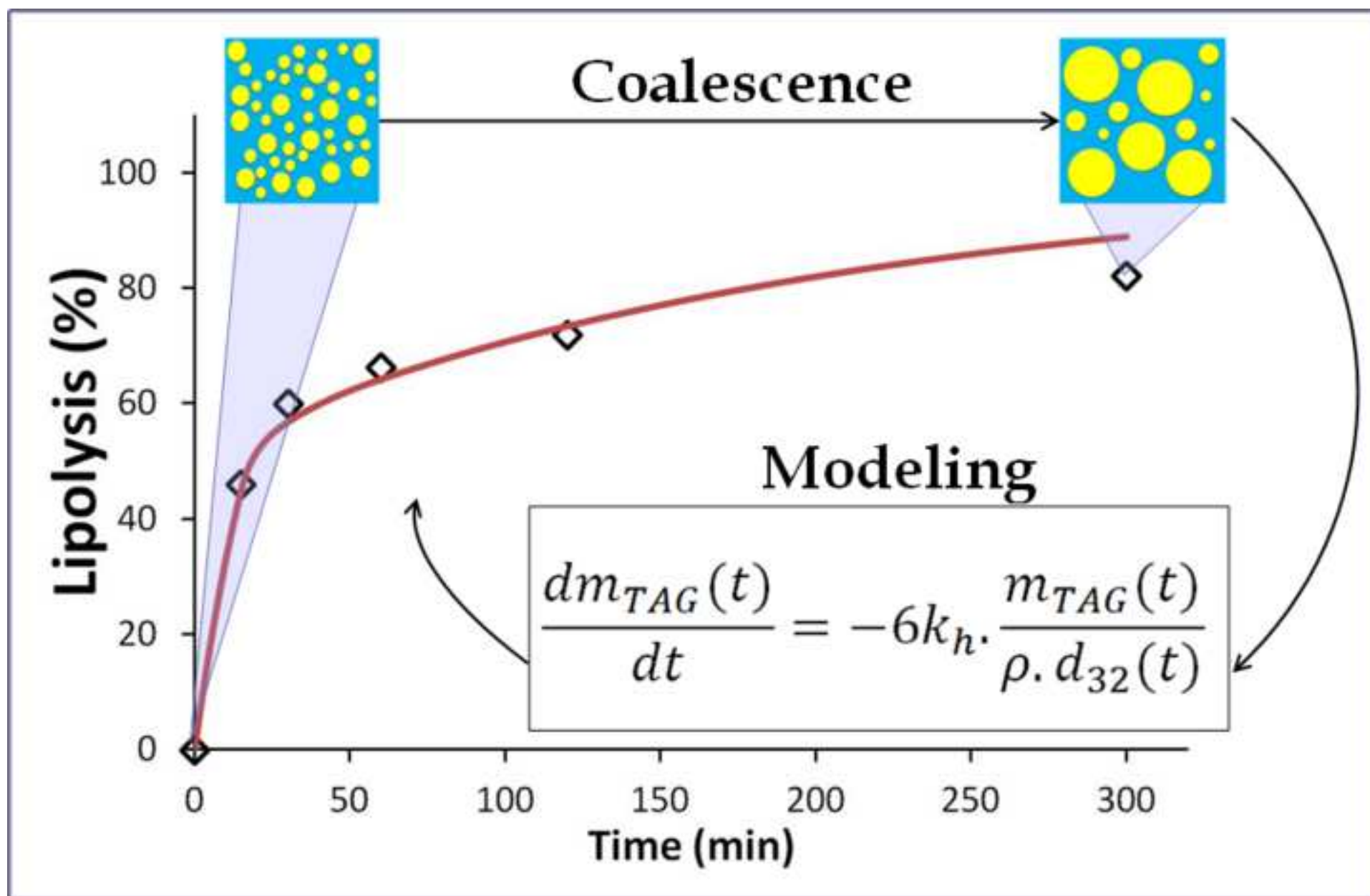
7
8 ¹ INRA, UMR782 Génie et Microbiologie des Procédés Alimentaires, F-78850 Thiverval
9 Grignon, France

10 ² AgroParisTech, UMR782 Génie et Microbiologie des Procédés Alimentaires, F-78850
11 Thiverval Grignon, France

12 ³ INRA, UR1268 Biopolymères Interactions Assemblages, F-44300 Nantes, France

13

14 *Corresponding author: steven.le-feunteun@grignon.inra.fr, +33(0)13814596



Highlights:

- A whey protein stabilized emulsion was submitted to *in vitro* digestion.
- The kinetics of pancreatic lipolysis plateaued after ~ 30 min of intestinal digestion.
- A marked coalescence of the oil droplets occurred concurrently.
- A mathematical model was developed and successfully used to relate both sets of data.
- Droplet coalescence, and not enzyme inhibition, was the key mechanism explaining the rate of lipid digestion.

15 **Abstract**

16 Whey protein stabilized submicron oil-in-water emulsions have been reported to remain
17 relatively stable in size during the gastric phase and to coalesce during the intestinal phase of
18 *in vitro* digestion experiments. The aim of this study was to understand the impact of oil
19 droplet coalescence on the intestinal lipolysis kinetics during an *in vitro* digestion of such
20 emulsion, and to develop a mathematical model able to predict the experimental observations.
21 A submicron whey protein stabilized emulsion made of a mixture of medium-chain (MCT)
22 and long-chain triacylglycerols (LCT) was prepared and submitted to gastro-intestinal *in vitro*
23 digestion. Triacylglycerol concentrations and droplet size distributions were measured before
24 and after the gastric phase and during the intestinal phase using HPLC and laser granulometry,
25 respectively. MCT were fully digested within 15 min of intestinal digestion, whereas LCT
26 were still detected after 5 hours. Moreover, the intestinal lipolysis of LCT showed a two-stage
27 behavior with an initial fast rate that markedly slowed down after about 30 min, a time at
28 which a sudden rise in the droplet sizes, attributed to coalescence, was also observed. A
29 mathematical model based on the experimentally measured droplet sizes and assuming a rate
30 of lipolysis proportional to the interfacial area was developed and successfully used to
31 reproduce the observed kinetics. Our results support the idea that droplet coalescence during
32 the intestinal phase was the main reason for the marked slowdown of the kinetics of lipid
33 digestion, hence suggesting that inhibition of the lipolysis reaction could be a secondary
34 factor only.

35

36 **Keywords:** Pancreatic lipase, Lipid digestion, Droplet size, Polyunsaturated Fatty Acids,
37 Simulation.

38 **1. Introduction**

39 Key parameters that govern food digestion *in vivo* are very hard to identify for practical
40 reasons. *In vitro* methods, for which the conditions are strictly controlled, have therefore been,
41 and are still, largely used. Concerning the digestion of emulsified lipids, both their
42 compositional and structural properties can affect digestion [1]. It is known that short chain
43 fatty acids are released faster and to greater extents than long-chain fatty acids [2-6], and that
44 polyunsaturated fatty acids such as docosahexanoic acid (DHA) and eicosapentaenoic acid
45 (EPA) are highly resistant to lipolysis [7-8]. The composition and the surface area of the
46 interface surrounding lipids are also very important parameters because digestive lipases must
47 adsorb on the droplet surface to reach their substrates. On the one hand, the kinetics of
48 lipolysis increases with the interfacial area, and hence with decreasing droplet sizes [3, 5-6, 9-
49 10]. On the other hand, the rate of the reaction depends on the lipase affinity for the interfacial
50 layer and may therefore be modulated by the nature of the emulsifiers used to stabilize the
51 emulsions [11-12].

52 Moreover, if lipid digestion is initiated in the stomach by the gastric lipase, most of the
53 reaction (70-90%) is performed in the upper part of the intestine by the combined action of
54 the pancreatic lipase, its colipase, and bile salts [1]. Beyond the properties of the native
55 emulsions, the structural modifications they may undergo within the stomach will affect the
56 intestinal phase, and hence the overall kinetics of the digestion [13]. Emulsions can remain
57 stable, flocculate or coalesce during the gastric phase depending on several parameters such
58 as the initial droplet size, the type of emulsifiers, and the composition of the surrounding
59 medium [14-17]. The rate of lipid hydrolysis during the intestinal phase can thus be impacted
60 by changes in the droplet surface area induced by the gastric structuring of the emulsions: the
61 lower the interfacial area when emptied into the duodenum, the slower the digestion. The

62 stability of the oil droplets against flocculation and coalescence in the stomach is therefore
63 essential to understand why two resembling emulsions may lead to different digestion kinetics.
64 Several studies have also highlighted that some emulsions can remain relatively stable during
65 the gastric phase but undergo important modifications during the intestinal phase of digestion.
66 Whey protein stabilized submicron emulsions are good examples thereof. They have been
67 reported to remain stable in size or flocculate in simulated gastric conditions [14, 18-19]. In
68 either case, the initial rate of lipolysis during the subsequent intestinal phase was fast and
69 comparable to other gastric stable emulsions [14], suggesting that flocculation during the
70 gastric step did not alter much the intestinal lipolysis kinetics. In parallel, other studies have
71 shown that whey protein stabilized emulsions are highly prone to coalescence during the
72 intestinal phase of *in vitro* digestion [11, 13, 19-20]. The effect of such an intestinal
73 coalescence of the oil droplets on the kinetics of pancreatic lipolysis have, however, not been
74 investigated so far.

75 Therefore, our study aimed at studying and modeling the influence of droplet coalescence on
76 the kinetics of pancreatic lipolysis during an *in vitro* gastrointestinal digestion of a whey
77 protein stabilized emulsion. The emulsion was prepared from a blend of medium-chain
78 triacylglycerols and a microalgae oil rich in docosahexaenoic acid (DHA), a long-chain ω 3
79 polyunsaturated fatty acid which daily recommended intake is 250 mg [21]. The evolution of
80 both the oil droplet sizes and the lipolysis kinetics were monitored throughout gastro-
81 intestinal *in vitro* digestion experiments. A mathematical model, in line with previously
82 published ones [5, 22-23], was developed to quantitatively evaluate the relationships between
83 the intestinal lipolysis kinetics and the evolution of the droplet surface area.

84 **2. Material and methods**

85 **2.1 Materials**

86 The oil containing medium-chain triacylglycerols (Miglyol 812S) (MCT): C8:0 (54%) and
87 C10:0 (43%) was purchased from Sasol GmbH, Germany. The oil containing long-chain
88 triacylglycerols (DHAsco) (LCT): docosahexaenoic acid (DHA, C22:6 n-3, 40%), C12:0
89 (4%), C14:0 (12%), C16:0 (12%) and C18:1 n-9 (24%) was obtained from Martek, via DSM
90 Nutritional Products Ltd, Switzerland. Whey protein powder (Prolacta 95) was purchased
91 from Lactalis Ingredients, France. Pepsin (P7012), mucin (M2378), pancreatin (P7545),
92 pancreatic lipase (L3126) and bile extract (B8631) were from porcine origin and obtained
93 from Sigma-Aldrich, France. Water was Milli-Q water. Solvents for liquid chromatography
94 were chloroform for HPLC (Carlo Erba), methyl alcohol for HPLC (99.9%, Carlo Erba),
95 ammonia solution (30%, Carlo Erba).

96

97 **2.2. Emulsion preparation**

98 An emulsion composed of 80% of aqueous phase and 20% of oil (w/w) was made. The
99 aqueous phase was prepared by dissolving 4% (w/w) of whey protein powder, used as
100 emulsifier, in a 0.1M sodium phosphate buffer at pH 7.0. The oil phase consisted of 62.5%
101 LCT and 37.5% MCT (w/w) mixed together. A rotor-stator homogenizer (SilentCrusher M
102 equipped with the 12F generator from Heidolph Instruments, Germany) was used in a pre-
103 emulsification step (5 min, 20000 rpm). The coarse emulsion was successively homogenized
104 for 5 min at 500 bars and for 10 min at 1000 bars under nitrogen flow with a high-pressure
105 homogenizer (C3-EmulsiFlex, Sodexim SA, France) temperature-controlled at 4°C to produce
106 the emulsion with droplet diameters below micron. A 50% (w/w) maltodextrin in water
107 solution was then added as a 1:1 (v/v) ratio to the emulsion and the mixture was thereafter
108 freeze-dried. The dried emulsion was then conditioned in oxygen hermetic bag under vacuum

109 and kept at -20°C until uses. The dried emulsion was rehydrated in Milli-Q water to obtain a
110 final oil concentration of 3.2% (w/w) on the day of the *in vitro* experiments.

111

112 **2.3 Emulsion digestion**

113 3 mL of the rehydrated emulsion, corresponding to an oil mass of about 96 mg, was placed
114 into 22.4 mL headspace vials hermetically sealed with Teflon/silicon septa and aluminum
115 caps. These vials were kept in a temperature controlled chamber at 37°C under magnetic
116 stirring ($400\text{ rpm}\cdot\text{min}^{-1}$) throughout the duration of the experiments. The gastric phase
117 duration was 60 min and was launched by adding 2.12 mL of simulated gastric fluid (SGF)
118 and $40\ \mu\text{L}$ of 1M HCl to reach a final pH of 2.5 in the reaction vials. The SGF solution
119 contained $3.9\ \text{g}\cdot\text{L}^{-1}$ of pepsin, $2.4\ \text{g}\cdot\text{L}^{-1}$ of mucin, 120 mM of NaCl, 2 mM of KCl and 6 mM
120 of CaCl_2 . The intestinal phase duration was then launched for 300 min maximum by adding
121 $4.86\ \text{mL}$ of simulated intestinal fluid (SIF) into the vials and $100\ \mu\text{L}$ of 1M NaCO_3 to reach a
122 final pH of 6.5. The simulated intestinal fluid (SIF) contained $30.8\ \text{g}\cdot\text{L}^{-1}$ of bile extract
123 powder, $0.82\ \text{g}\cdot\text{L}^{-1}$ of pancreatin, $0.41\ \text{g}\cdot\text{L}^{-1}$ of pancreatic lipase, and the same electrolyte
124 concentrations as the SGF.

125 The native emulsion (NE), and samples taken at the end of the gastric phase (G60), at $t = 0$
126 min of the intestinal phase (I0) using a modified SIF that contained all constituents except
127 pancreatin and lipase, and at 15, 30, 60, 120 and 300 min of intestinal digestion (I15 to I300)
128 were analyzed. One vial was used for one sampling time and one type of measurement
129 (quantification of LCT and MCT by HPLC or droplet size by laser granulometry) so that the
130 contents of 16 vials were analyzed in total (2 methods times 8 sampling times) for one
131 digestion. Three independent digestion experiments, further denoted replicates, were
132 performed. Samples devoted to droplet size measurements were analyzed immediately,
133 whereas samples devoted to HPLC measurements were kept at -80°C until further analysis.

134

135 **2.4 Quantification of LCT and MCT by HPLC**

136 HPLC paired with an evaporative light scattering detector (ELSD) was used to quantify the
137 decrease of both LCT and MCT masses during the time course of the *in vitro* digestions. Total
138 lipids were extracted from 1.5 mL of the native emulsions or of the stomach media and from 3
139 mL of the intestinal media according to the Bligh and Dyer [24] procedure with minor
140 modifications in the ratio $\text{CHCl}_3/\text{CH}_3\text{OH}/\text{H}_2\text{O}$ 1/2/1. Before the HPLC analyses, the lipid
141 extract was dissolved in CHCl_3 down to $0.3 \text{ mg}\cdot\text{mL}^{-1}$ for native emulsion and stomach media
142 and to $0.7 \text{ mg}\cdot\text{mL}^{-1}$ for intestinal media. HPLC operating conditions were similar to those
143 described in [25] using a Uptip-prep Strategy column ($2.2 \mu\text{m SI}$, $150\times 4.6 \text{ mm}$, Interchim,
144 Montluçon, France) and $30 \mu\text{L}$ of injected lipid extract. As illustrated in **Fig. 1**, injected
145 masses of pure MCT and LCT ranging from 0.5 to $9 \mu\text{g}$ led to a power law calibration curve
146 with no distinction of the TAG chain-length.

147 The triacylglycerol region of an HPLC chromatogram stemming from an undigested sample is
148 presented in **Fig. 2**. The retention times of LCT (1.21 min) and MCT (1.32 min) were
149 different but their signals partly overlapped. As illustrated in **Fig. 2**, signal deconvolution was
150 therefore undertaken using a specifically developed algorithm running with the Matlab™
151 software (The MathWorks Inc., Natick, MA) and the recovered LCT and MCT signals were
152 converted into masses using the calibration curve (**Fig. 1**). Reliable results were obtained
153 using this procedure as shown from the comparison of the mean LCT and MCT masses of
154 57.3 ± 2.7 and $35.0 \pm 2.0 \text{ mg}$ (estimated over 15 undigested samples) with the 59.7 and 35.7
155 mg targeted masses in each digestion vial, respectively. LCT and MCT masses were finally
156 converted into lipolysis percentages using **Eq. 1**:

$$\text{lipolysis}(t) = \frac{m_{TAG_0} - m_{TAG}(t)}{m_{TAG_0}} \times 100 \quad (1)$$

157 where m_{TAG_0} and $m_{TAG}(t)$ are the masses (mg) of LCT or MCT initially present in the vials
158 and measured by HPLC at time t, respectively.

159

160 **2.5 Droplets size measurement**

161 The volume-based distribution of oil droplet sizes was measured using a Mastersizer S
162 (Malvern Instruments Ltd., Worcestershire, UK) equipped with a 2 mW He-Ne laser of $\lambda =$
163 633 nm and the 300RF lens with detection limits of 0.05 and 900 μm . The refractive index n_0
164 of the aqueous phase was 1.33 and the properties of the dispersed phase were 1.457 for the
165 refractive index and 0.001 for the absorption. Samples were pre-diluted 100-fold with the
166 desired solution (with or without sodium dodecyl sulfate, SDS, as deflocculating agent), and
167 then diluted with distilled water to reach an oil volume concentration near 0.01% for the
168 circulation in the measurement cell. All analyses were performed at room temperature as
169 described previously [8, 25]. The surface-weighted mean diameter, d_{32} , corresponding to the
170 droplet diameter having the same ratio of volume to surface area as the droplet distribution,
171 was calculated according to:

$$d_{32} = \frac{\sum_i n_i d_i^3}{\sum_i n_i d_i^2}$$

172 where n_i is the number of droplets of diameter d_i .

173

174 **3. Mathematical modeling**

175 **3.1 Model assumptions and equations**

176 Lipolysis is mediated by the pancreatic colipase-lipase system which absorbs onto the droplet
177 interface and splits the *sn*-1 and *sn*-3 ester bonds of triacylglycerols (TAG). The first step of
178 the reaction generates one free fatty acid (FFA) and a diacylglycerol (DAG) which is further
179 transforms into a second FFA and the *sn*-2-monoacylglycerol. Our model simulates the

180 kinetics of lipolysis as inferred from the disappearance of the TAG molecules so that, in
 181 principle, it only characterizes the first step of the reaction. Nevertheless, the lack of detected
 182 DAG in the course of the experiments strongly suggests that the second reaction step was not
 183 rate-limiting in our experimental conditions, and hence that similar lipolysis kinetics would
 184 have been recovered by monitoring the appearance of the final products of the reaction. The
 185 main modeling assumptions were as follows:

186 A1: The rate of TAG hydrolysis was assumed proportional to the interfacial area of the
 187 droplets [13-14, 22]. This means that the surface reaction rate was taken as constant in the
 188 considered experimental conditions. Thus:

$$\frac{dm_{TAG}(t)}{dt} = -k_h \cdot A(t) \quad (2)$$

189 where k_h is the hydrolysis rate constant ($\text{mg} \cdot \text{m}^{-2} \cdot \text{min}^{-1}$) and $A(t)$ is the interfacial area (m^2) at
 190 time t (min).

191 A2: The droplets were considered as spheres, and the interfacial area of the droplets was
 192 assumed to be adequately described by the size distributions measured by laser granulometry
 193 and their corresponding d_{32} . Hence, one can write that:

$$A(t) = 6 \frac{V_{TAG}(t)}{d_{32}(t)} \quad (3)$$

194 where $d_{32}(t)$ is the surface-weighted mean diameter (nm) at time t , and $V_{TAG}(t)$ is the
 195 volume of TAG in the sample (mm^3) at time t . **Eq. 3** can be further transformed into:

$$A(t) = 6 \frac{m_{TAG}(t)}{\rho \cdot d_{32}(t)} \quad (4)$$

196 where ρ is the mass density of TAG (mg/mm^3) and $m_{TAG}(t)$ is the mass of TAG (mg) at time
 197 t .

198 Combining **Eq. 1** and **4**, the evolution of the TAG mass is given by:

$$\frac{dm_{TAG}(t)}{dt} = -6k_h \cdot \frac{m_{TAG}(t)}{\rho \cdot d_{32}(t)} \quad (5)$$

199 To solve the differential equation **Eq. 5**, one also needs to know how the droplet sizes evolve
200 as a function of time. In the present study, we resorted to two different assumptions on $d_{32}(t)$,
201 leading to two different versions of the model:

202 A3a: In one version, it was assumed that all droplets had the same diameter and that the total
203 number of droplets remained constant, hypotheses that lead to the following equation [5]:

$$d_{32}(t) = d_0 \sqrt[3]{\frac{m_{TAG}(t)}{m_{TAG_0}}} \quad (6)$$

204 where m_{TAG_0} is the mass of TAG initially introduced in the reaction vial and d_0 is the droplet
205 diameter of the native emulsion.

206 A3b: In the other version, $d_{32}(t)$ was estimated by linear interpolations of the experimental
207 values recovered using laser granulometry.

208 For both model versions, the masses calculated by solving **Eq. 5** were finally converted into
209 percentages of lipolysis using **Eq. 1** to enable the comparison of the model simulations with
210 experimental data.

211

212 **3.2 Model fitting and parameter estimation**

213 The lipolysis of MCT was so fast that it was already finished at $t = 15$ min, *i.e.* the first
214 sampling time. Only the lipolysis of LCT was therefore considered to confront the model to
215 the experimental data. The differential equation **Eq. 5** was numerically solved using a LCT
216 mass density, ρ , of 0.92 g.cm^{-3} , and each of the previously described assumptions (A3a or b)
217 for the droplet size evolution as a function of time, $d_{32}(t)$. The unknown hydrolysis rate, k_h ,
218 was then estimated by fitting model predictions to the LCT lipolysis results determined by
219 HPLC. The recovered value, expressed in mg of TAG per minute and square meter of
220 interfacial area ($\text{mg.m}^{-2}.\text{min}^{-1}$), was then converted into $\mu\text{mol.m}^{-2}.\text{min}^{-1}$ for comparison

221 purposes with the literature using a LCT molar mass of $900 \text{ g}\cdot\text{mol}^{-1}$. Numeric calculations
222 were performed using Matlab™ software (The MathWorks Inc., Natick, MA).

223

224 **4. Results and Discussion**

225 **4.1 Kinetics of lipolysis of LCT and MCT**

226 The evolution of HPLC chromatograms during the intestinal phase stemming from one *in*
227 *vitro* digestion experiment is shown in **Fig. 3A**, and the mean percentages of lipolysis
228 calculated over the three replicates are presented in **Fig. 3B**. Initially, 2 peaks were clearly
229 visible in the chromatograms. The signal of the native emulsion and at $t = 0$ min of the
230 intestinal phase (modified SIF with no lipase) were similar since no gastric lipase was used in
231 this study. At $t = 15$ min of intestinal digestion, the signal arising from MCT entirely
232 disappeared, indicating that MCT were fully hydrolyzed in only few minutes. In contrast,
233 about 20% of the initial LCT mass was still detected after 300 min (*i.e.* 5h) of intestinal
234 digestion, showing that lipolysis was much slower for LCT than for MCT (**Fig. 3B**). In fact,
235 lipolysis of LCT was relatively fast during the first 30 minutes of digestion but was greatly
236 slowed down afterwards, resulting in a two-stage curve typical of most *in vitro* lipolysis
237 studies on submicron emulsions made of long-chain triacylglycerols [4-5, 14].

238 Higher rates of lipolysis of MCT compared to LCT have been reported in many studies using
239 pure MCT and LCT emulsions or MCT/LCT mixed emulsions as in the present study [2-5].
240 This is generally attributed to the higher water solubility of medium-chain FFAs than long-
241 chain FFAs. Indeed, the low water solubility of long-chain FFAs would lead to their
242 accumulation at the interface that would, in turn, inhibit the lipase activity by steric hindrance
243 until they are removed by bile salts or by forming soap with calcium ions [26]. In contrast, the
244 higher water solubility of medium-chain FFAs would facilitate their release from the interface,
245 and hence promote further hydrolysis of triacylglycerols at the droplet surface. According to

246 the composition of our emulsion, other factors may also have contributed to the higher rate of
247 MCT hydrolysis. Indeed, it has been reported that triacylglycerols containing
248 docosahexaenoic acid are more resistant to pancreatic lipase [7], possibly because of an
249 inhibitory effect induced by the presence of a double bond near the carboxyl group. For
250 MCT/LCT mixed emulsions, it has also been shown that MCT hydrolysis can be promoted to
251 the detriment of that of LCT [2] because of a preferential location, or turnover, of MCT at the
252 droplet interface [2-3]. It is therefore likely that different mechanisms have contributed to the
253 marked difference we observed in the lipolysis kinetics of MCT and LCT.

254

255 **4.2 Evolution of the droplet size**

256 The evolution of the particle size distribution (measured without deflocculating agent)
257 stemming from one *in vitro* digestion experiment is shown in **Fig. 4A**. The native emulsion
258 (NE) presented a monomodal distribution with a mean d_{32} of 0.26 μm . The mean size
259 increased considerably during the gastric phase since the measured d_{32} was $3.00 \pm 0.46 \mu\text{m}$
260 after 60 min of contact with the SGF (G60). However, the size distribution and the measured
261 d_{32} returned close to their original values after dilution of the same sample in a 1% SDS
262 solution (not shown) or after addition of a SIF with no pancreatin or lipase (I0). This
263 demonstrates that the increase of the mean diameter during the gastric phase was caused by
264 droplet flocculation, and that the subsequent addition of bile led to a deflocculation of these
265 droplet aggregates. During the intestinal phase, the droplet size distribution remained similar
266 during the first 15 min (I15). It was suddenly shifted toward considerably larger diameters at
267 about $t = 30$ min (mean volume diameter of about 9 μm) and remained relatively stable until
268 the end of the experiment (I30 to I300), with a good repeatability of the surface weighted
269 diameters over the three replicates (**Fig. 4B**).

270 According to the demonstrated tendency of bile to deflocculate the droplet aggregates formed
271 during the gastric phase, the increase of the particle size during the intestinal phase most
272 assuredly resulted from a coalescence of the oil droplets. This conclusion is moreover
273 consistent with previous studies showing that whey protein stabilized submicron emulsions
274 undergo coalescence during *in vitro* intestinal digestion [11, 13, 19-20]. We may even
275 highlight that the evolution of the size distributions we measured is highly similar to previous
276 results obtained during the digestion of a whey protein stabilized soya oil emulsion with an
277 initial d_{32} of 0.37 μm , and for which an intense coalescence was observed by confocal
278 microscopy after 10 to 30 min of intestinal digestion [19]. Hence, even if flocculation cannot
279 be totally excluded from our own set of data, we will only refer to the term of coalescence in
280 the rest of this article.

281 We may also highlight the remarkable simultaneity of the increase of the droplet size (**Fig. 4B**)
282 and of the decrease of the lipolysis rate (LCT in **Fig. 3B**). Although the authors did not point
283 out this particular aspect, it seems that droplet coalescence during the intestinal phase was
284 also concomitant with a decrease of the lipolysis rate in the recent study of Li and coworkers
285 [19]. It is indeed well known that the rate of lipolysis decreases with decreasing surface area,
286 and hence with increasing droplet size [3, 14, 16, 22, 27]. We can therefore wonder how
287 much of the decrease of the LCT lipolysis kinetics at about $t = 30$ min (**Fig. 3B**) was induced
288 by droplet coalescence. This was further explored using a modeling approach.

289

290 **4.3 Modeling results**

291 We remind that MCT was fully hydrolyzed in less than 15 min so that only LCT lipolysis was
292 considered for the modeling. The results obtained with three different mathematical models
293 are presented in **Fig 5A**. First, the dotted line represents our model version that assumes a
294 constant number of droplets of identical diameter (assumption A3a), and which decreases in

295 size upon hydrolysis of the TAG they contain (**Fig. 5B**). The fit was very bad because the
296 assumed mechanisms could not reproduce the strong decrease of the reaction kinetics at about
297 30 min.

298 Second, the dashed line represents the model proposed by Li and McClements [5]. This model
299 is similar to the previous one but further assumes that a fraction of the TAG can remain
300 undigested. It provided a very good fit of our experimental data ($R^2 = 0.9888$) and led to a
301 lipolysis extent of $77.3 \pm 2.6 \%$ and a surface rate constant (k_h) of $9.4 \pm 1.5 \mu\text{mol.m}^{-2}.\text{min}^{-1}$,
302 which is rather close to the $13.8 \mu\text{mol.m}^{-2}.\text{min}^{-1}$ reported for a corn oil emulsion in [5]. As
303 noticed by the authors, these rate constants should nevertheless be considered as upper values
304 whenever droplet flocculation or coalescence takes place because, in such cases, the model
305 would not adequately simulate the evolution of the available interfacial area. This is also why
306 the mean diameter simulated with this model decreased from 350 to 213 nm (**Fig. 5B**), a trend
307 that is not consistent with our experimental results (**Fig. 4**).

308 Finally, the solid line represents our model version that accounts for the experimentally
309 measured d_{32} (**Fig. 5A and B**). This model also reproduced the experimental data very well
310 ($R^2 = 0.9882$). The underlying interpretation is however entirely different since the marked
311 slowdown of the reaction kinetics around 30 min is here fully explained by the decrease of the
312 interfacial area caused by droplet coalescence (*i.e.* no upper fraction of the digested lipids is
313 assumed here). The only unknown parameter in this model is the surface reaction rate (k_h)
314 that was estimated to be $2.4 \pm 0.1 \mu\text{mol.m}^{-2}.\text{min}^{-1}$.

315 To support the above considerations, the interfacial surface area was calculated for both our
316 model accounting for coalescence and the model of Li and McClements (**Fig. 6**). According
317 to the model of Li and McClements, the droplet size reduces upon TAG hydrolysis, leading to
318 a corresponding decrease of the surface area. The lipolysis nevertheless plateaued (**Fig. 5A**)
319 despite a large remaining droplet surface area. This suggests that the interface was no more

320 available for the enzymatic action, or in other words, that the reaction was inhibited by a
321 mechanism such as an accumulation of the reaction products at the droplet surface. According
322 to our model however, the slowdown of lipolysis was clearly, and solely, related to the sharp
323 decrease of the interfacial area induced by droplet coalescence. At 300 min, the available
324 interfacial area was low but nonzero, in agreement with the fact that lipolysis still proceeded
325 slowly. Note also that the reaction rate constants estimated with both models reflect these
326 differences of simulated surface area since they are expressed per unit of interfacial area. This
327 is indeed why the value recovered using our model (assumption A3b) is about 4 times smaller
328 than the value estimated with the model of Li and McClements (2.4 and $9.4 \mu\text{mol}\cdot\text{m}^{-2}\cdot\text{min}^{-1}$,
329 respectively).

330 Taking into account the evolution of the experimentally measured droplet sizes, the
331 mathematical model allowed a good prediction of the intestinal lipolysis kinetics. The
332 decrease of the interfacial area was thus the major reason for the slowdown of the reaction
333 rate after about 30 min. We may even highlight that our model slightly overestimates the last
334 experimental point of the kinetics at $t = 300$ min (**Fig. 5A**). Thus, our results are still
335 compatible with an inhibition of the enzymatic reaction at the interface, but as a second order
336 factor.

337 On the one hand, our results confirm that the kinetics of lipolysis are essentially proportional
338 to the interfacial area [22]. On the other hand, they may also offer a complementary
339 explanation for the strong decreases of the lipolysis kinetics that are frequently observed after
340 few minutes of intestinal *in vitro* digestions. Indeed, such slowdowns are often attributed to an
341 inhibition induced by the reaction products that accumulate at the interface, with no or little
342 attention given to a possible coalescence or flocculation of the emulsion droplets. This is most
343 probably because such phenomena have not been expected to occur in the conditions
344 encountered in the intestinal phase because of high concentrations of bile salts and no

345 macroscopic visual evidences. Nevertheless, several recent studies have shown that droplet
346 flocculation and coalescence might in fact be encountered during the intestinal phase of *in*
347 *vitro* experiments [11, 13, 17, 19-20], similarly to what has now been established for the
348 gastric phase [14, 16-17].

349 The exact cause for the occurrence of coalescence still remains to be studied because the
350 nature of the interfacial layer is continuously evolving, especially in the case of protein-
351 stabilized emulsion. The TAG composition of the droplets is evolving in the course of the
352 reaction [28] and a competitive adsorption process takes place at the interface between
353 emulsifier molecules, enzymes, bile salts and the products of the lipolysis reactions. It has
354 been reported that hydrolysis of the proteins adsorbed at the interface can weaken the droplet
355 repulsion forces and favor droplet flocculation or coalescence [19, 25], possibly explaining
356 why protein stabilized emulsions seem more sensitive to these phenomena [27]. Droplet
357 coalescence during digestion has also been reported to be promoted by the accumulation of
358 monoacylglycerols and fatty acids at the interface [16, 28], that is, by the same mechanism as
359 that usually put forward to support an inhibition of the enzymatic reaction. More studies are
360 therefore needed to determine the frequency of droplet coalescence during *in vitro* intestinal
361 digestions and to better understand its consequences on the lipolysis kinetics.

362

363 **5. Conclusion**

364 Our study confirms previously reported results showing that the kinetics of lipolysis is much
365 faster for MCT than for LCT when they are mixed together in the same emulsion. In
366 agreement with recent studies, it also confirms that whey protein stabilized submicron
367 emulsions are prone to coalescence during the intestinal phase of *in vitro* digestions.
368 Moreover, by accounting for the experimentally measured droplet distributions in a modeling
369 approach, we were able to adequately reproduce the two-stage lipolysis curve recovered for

370 LCT with an initial fast reaction rate that markedly slowed down after about 30 min. These
371 modeling results demonstrate that droplet coalescence had a considerable impact on the
372 lipolysis kinetics of the remaining LCT by causing a sharp reduction of the interfacial area
373 available for the adsorption of pancreatic lipase-colipase. Contrarily to what is generally
374 postulated for intestinal lipid digestion, our findings suggest that inhibition of the enzymatic
375 reaction might not always be the key mechanism explaining why *in vitro* lipolysis kinetics of
376 emulsified lipids often plateaus before the reaction is completed.

377

378 **Acknowledgements**

379 The authors thank Valérie Beaumal (UR1268 BIA) for the preparation of the freeze-dried
380 emulsion and Claude Genot and Sebastien Marze for helpful remarks and discussions. This
381 work was supported by the Institut National de la Recherche Agronomique and the Institut
382 Carnot QUALIMENT (France). The authors are involved in the Food and Agriculture COST
383 (European Cooperation in Science and Technology) Action FA1005 ‘Improving health
384 properties of food by sharing our knowledge on the digestive process (INFOGEST)’,
385 <http://www.cost-infogest.eu>

386 **References**

- 387 1. Armand, M., *Lipases and lipolysis in the human digestive tract: where do we stand?*
388 Current Opinion in Clinical Nutrition and Metabolic Care, 2007. **10**(2): p. 156-164.
- 389 2. Deckelbaum, R.J., et al., *Medium-chain versus long-chain triacylglycerol emulsion*
390 *hydrolysis by lipoprotein-lipase and hepatic lipase - Implications for the mechanisms*
391 *of lipase action.* Biochemistry, 1990. **29**(5): p. 1136-1142.
- 392 3. Armand, M., et al., *Effects of droplet size, triacylglycerol composition, and calcium on*
393 *the hydrolysis of complex emulsions by pancreatic lipase - An in vitro study.* Journal
394 of Nutritional Biochemistry, 1992. **3**(7): p. 333-341.
- 395 4. Zhu, X., et al., *Free fatty acid profiles of emulsified lipids during in vitro digestion*
396 *with pancreatic lipase.* Food Chemistry, 2013. **139**(1-4): p. 398-404.
- 397 5. Li, Y. and D.J. McClements, *New mathematical model for interpreting pH-stat*
398 *digestion profiles: Impact of lipid droplet characteristics on in vitro digestibility.*
399 Journal of Agricultural and Food Chemistry, 2010. **58**(13): p. 8085-8092.
- 400 6. Li, Y., M. Hu, and D.J. McClements, *Factors affecting lipase digestibility of*
401 *emulsified lipids using an in vitro digestion model: Proposal for a standardised pH-*
402 *stat method.* Food Chemistry, 2011. **126**(2): p. 498-505.
- 403 7. Bottino, N.R., G.A. Vandenburg, and R. Reiser, *Resistance of certain long-chain*
404 *polyunsaturated fatty acids of marine oils to pancreatic lipase hydrolysis.* Lipids,
405 1967. **2**(6): p. 489-93.
- 406 8. Marze, S., A. Meynier, and M. Anton, *In vitro digestion of fish oils rich in n-3*
407 *polyunsaturated fatty acids studied in emulsion and at the oil-water interface.* Food &
408 Function, 2013. **4**(2): p. 231-239.

- 409 9. Armand, M., et al., *Emulsion and absorption of lipids: The importance of*
410 *physicochemical properties*. *Ocl-Oleagineux Corps Gras Lipides*, 1997. **4**(3): p. 178-
411 185.
- 412 10. Borel, P., et al., *Hydrolysis of emulsions with different triglycerides and droplet sizes*
413 *by gastric lipase in vitro - Effect on pancreatic lipase activity* *Journal of Nutritional*
414 *Biochemistry*, 1994. **5**(3): p. 124-133.
- 415 11. Mun, S., E.A. Decker, and D.J. McClements, *Influence of emulsifier type on in vitro*
416 *digestibility of lipid droplets by pancreatic lipase*. *Food Research International*, 2007.
417 **40**(6): p. 770-781.
- 418 12. Hur, S.J., E.A. Decker, and D.J. McClements, *Influence of initial emulsifier type on*
419 *microstructural changes occurring in emulsified lipids during in vitro digestion*. *Food*
420 *Chemistry*, 2009. **114**(1): p. 253-262.
- 421 13. Singh, H., A.Q. Ye, and D. Horne, *Structuring food emulsions in the gastrointestinal*
422 *tract to modify lipid digestion*. *Progress in Lipid Research*, 2009. **48**(2): p. 92-100.
- 423 14. Golding, M., et al., *Impact of gastric structuring on the lipolysis of emulsified lipids*.
424 *Soft Matter*, 2011. **7**(7): p. 3513-3523.
- 425 15. Marciani, L., et al., *Enhancement of intragastric acid stability of a fat emulsion meal*
426 *delays gastric emptying and increases cholecystokinin release and gallbladder*
427 *contraction*. *American Journal of Physiology-Gastrointestinal and Liver Physiology*,
428 2007. **292**(6): p. G1607-G1613.
- 429 16. Wooster, T.J., et al., *Impact of different biopolymer networks on the digestion of*
430 *gastric structured emulsions*. *Food Hydrocolloids*, 2014. **36**: p. 102-114.
- 431 17. Day, L., et al., *Tailoring the digestion of structured emulsions using mixed*
432 *monoglyceride-caseinate interfaces*. *Food Hydrocolloids*, 2014. **36**: p. 151-161.

- 433 18. Nik, A.M., A.J. Wright, and M. Corredig, *Surface adsorption alters the susceptibility*
434 *of whey proteins to pepsin-digestion*. Journal of Colloid and Interface Science, 2010.
435 **344**(2): p. 372-381.
- 436 19. Li, J., et al., *Physicochemical behaviour of WPI-stabilized emulsions in in vitro gastric*
437 *and intestinal conditions*. Colloids and Surfaces B-Biointerfaces, 2013. **111**: p. 80-87.
- 438 20. Sarkar, A., D.S. Horne, and H. Singh, *Pancreatin-induced coalescence of oil-in-water*
439 *emulsions in an in vitro duodenal model*. International Dairy Journal, 2010. **20**(9): p.
440 589-597.
- 441 21. EFSA, *Scientific opinion on dietary reference values for fats, including saturated fatty*
442 *acids, polyunsaturated fatty acids, monounsaturated fatty acids, trans fatty acids, and*
443 *cholesterol*. EFSA Journal, 2010. **8** (3): **1461**.
- 444 22. Verger, R. and G.H. De Haas, *Interfacial enzyme kinetics of lipolysis*. Annual Review
445 of Biophysics and BioEngineering, 1976. **5**: p. 77-117.
- 446 23. Jurado, E., et al., *Kinetics of the enzymatic hydrolysis of triglycerides in o/w emulsions:*
447 *Study of the initial rates and the reaction time course*. Biochemical Engineering
448 Journal, 2008. **40**(3): p. 473-484.
- 449 24. Bligh, E.G. and W.J. Dyer, *A rapid method of total lipid extraction and purification*.
450 Canadian Journal of Biochemistry and Physiology, 1959. **37**: p. 911-917.
- 451 25. Kenmogne-Domguia, H.B., et al., *Gastric conditions control both the evolution of the*
452 *organization of protein-stabilized emulsions and the kinetic of lipolysis during in vitro*
453 *digestion*. Food & Function, 2012. **3**(12): p. 1302-1309.
- 454 26. Zangenberg, N.H., et al., *A dynamic in vitro lipolysis model I. Controlling the rate of*
455 *lipolysis by continuous addition of calcium*. European Journal of Pharmaceutical
456 Sciences, 2001. **14**(2): p. 115-122.

- 457 27. Singh, H. and A.Q. Ye, *Structural and biochemical factors affecting the digestion of*
458 *protein-stabilized emulsions*. *Current Opinion in Colloid & Interface Science*, 2013.
459 **18**(4): p. 360-370.
- 460 28. Ye, A.Q., et al., *Effect of calcium on the kinetics of free fatty acid release during in*
461 *vitro lipid digestion in model emulsions*. *Food Chemistry*, 2013. **139**(1-4): p. 681-688.
462
463

1 **Fig 1.** Calibration curve relating the HPLC signal to the injected mass of TAG. The light
2 scattering detector responded the same way to both LCT (triangles) and MCT (diamonds).

3

4 **Fig 2.** HPLC chromatogram stemming from an undigested sample (circles) superimposed
5 with the results of the deconvolution process: LCT signal (dashed line), MCT signal (dotted
6 line) and their sum (solid line).

7

8 **Fig 3.** (A) Typical evolution of HPLC chromatograms during the intestinal phase of *in vitro*
9 digestion: native emulsion (dashed line) and, from top to bottom, at $t = 0, 15, 30, 60, 120$ and
10 300 min after the SIF addition, respectively. (B) Extent of lipolysis for MCT (diamonds) and
11 LCT (triangles) during the intestinal phase. Means and standard deviations (smaller than the
12 symbol size) were calculated over 3 replicates.

13

14 **Fig 4.** (A) Typical evolution of the droplet size distributions measured without deflocculating
15 agent during *in vitro* digestion. From back to front: Native emulsion (NE), samples taken at
16 the end of the gastric phase (G60), and at $t = 0, 15, 30, 60, 120$ and 300 min (I0 to I300) after
17 the SIF addition, respectively. (B) Evolution of the d_{32} during the intestinal phase. Means and
18 standard deviations (vertical bars) were calculated over 3 replicates.

19

20 **Fig 5.** (A) Extent of LCT lipolysis measured by HPLC (symbols) and the fits obtained with i)
21 our model that does not account for the observed coalescence (dotted line, assumption A3a), ii)
22 the model of Li and McClements [5] (dashed line), and iii) our model that accounts for
23 coalescence using the measured d_{32} (solid line, assumption A3b). (B) Comparison of the
24 measured (symbols) and simulated d_{32} for the different models (same line coding).

25

26 **Fig 6.** Evolution of the interfacial area during the intestinal phase according to our model that
27 accounts for coalescence using the measured d_{32} (solid line, assumption A3b) and to the
28 model of Li and McClements [5] (dashed line).

29

Figure1

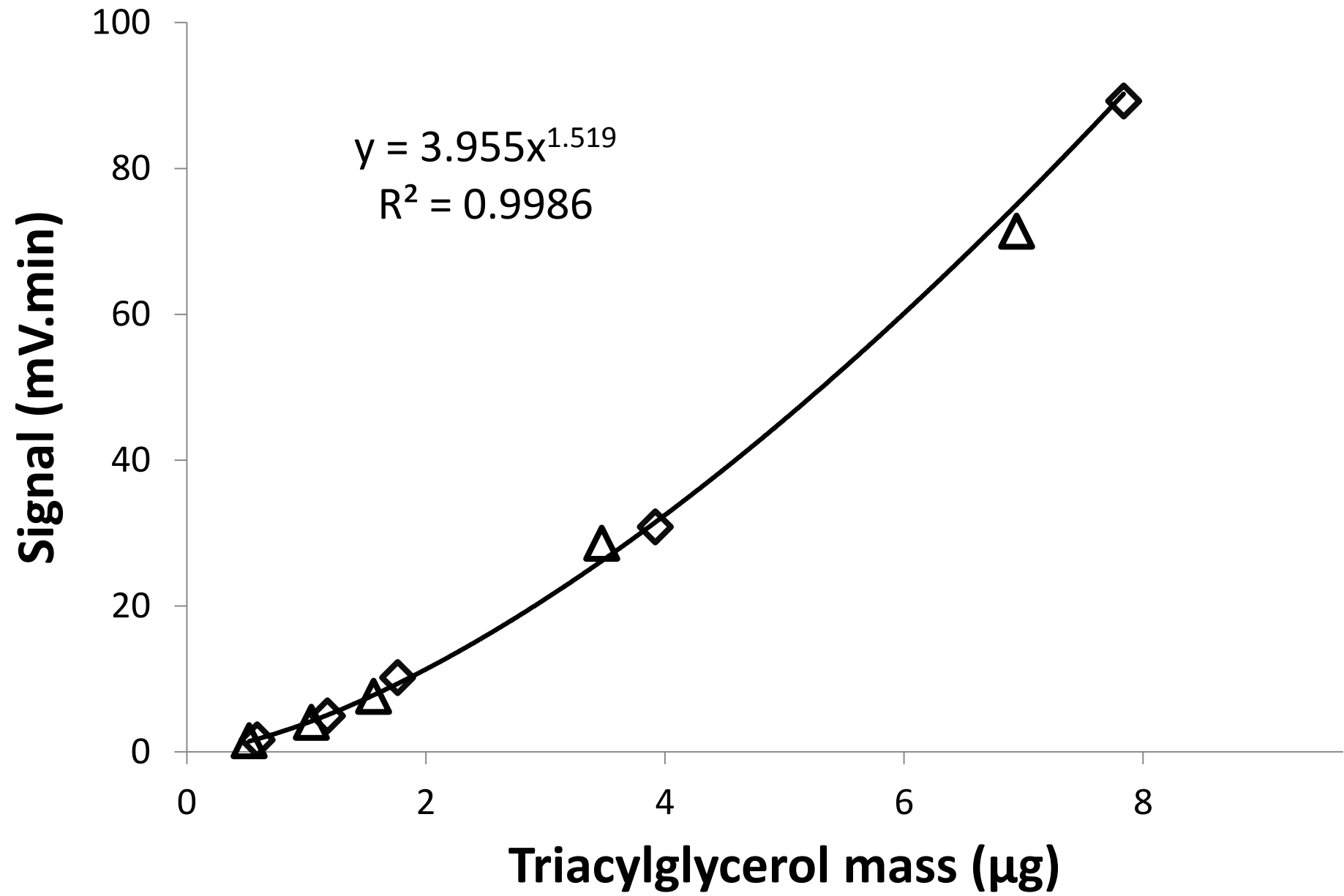


Figure2

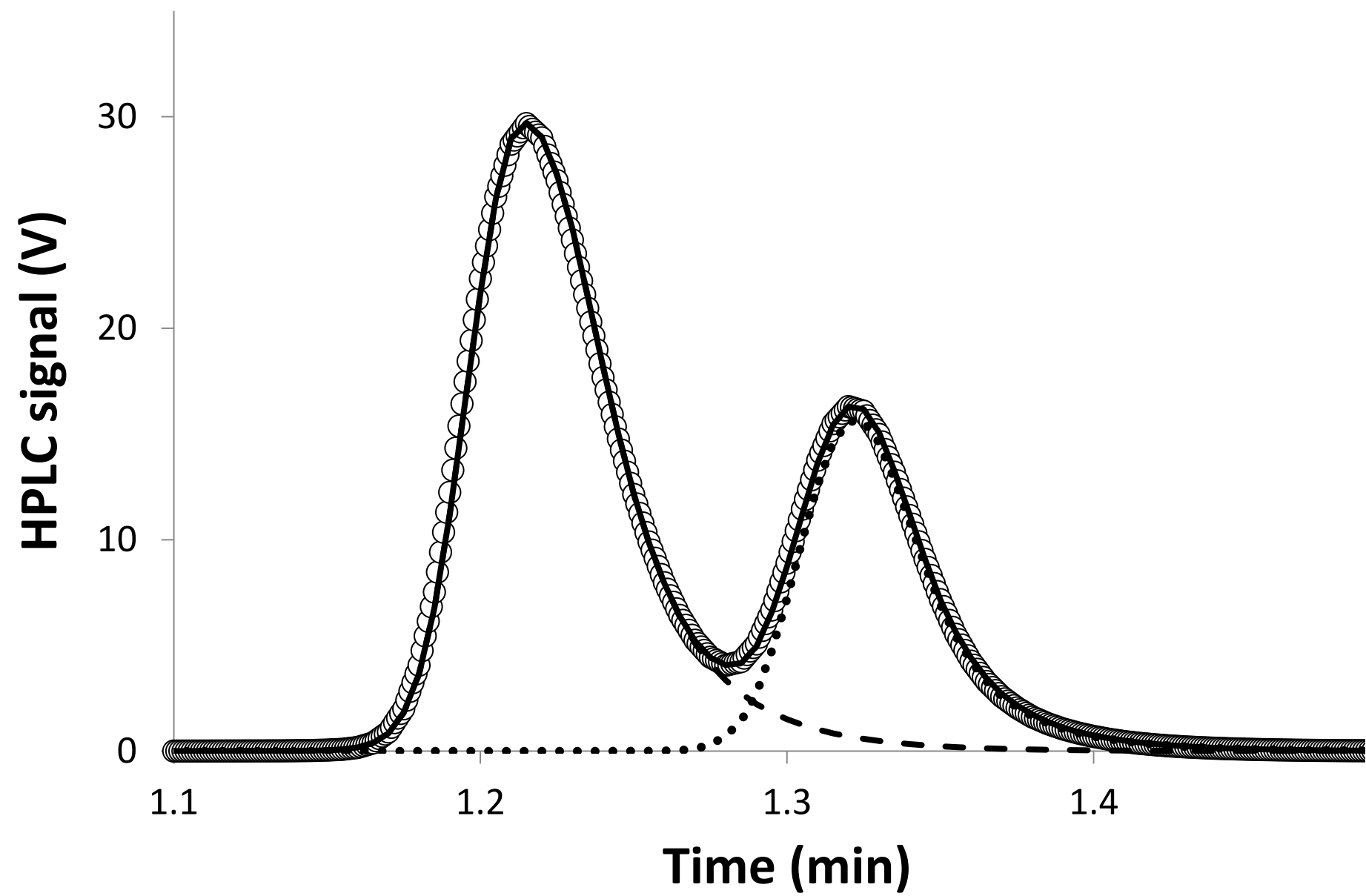


Figure3

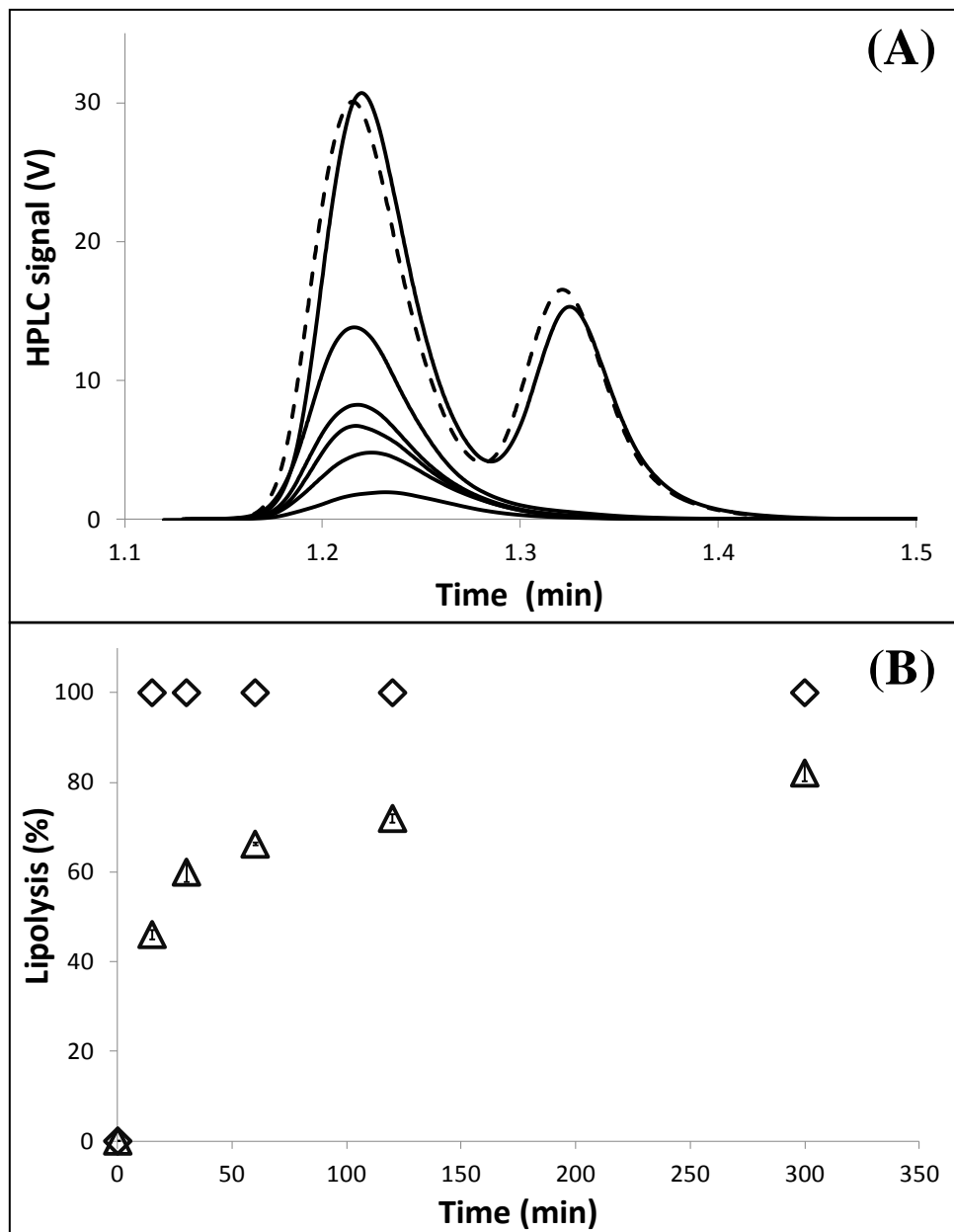


Figure4

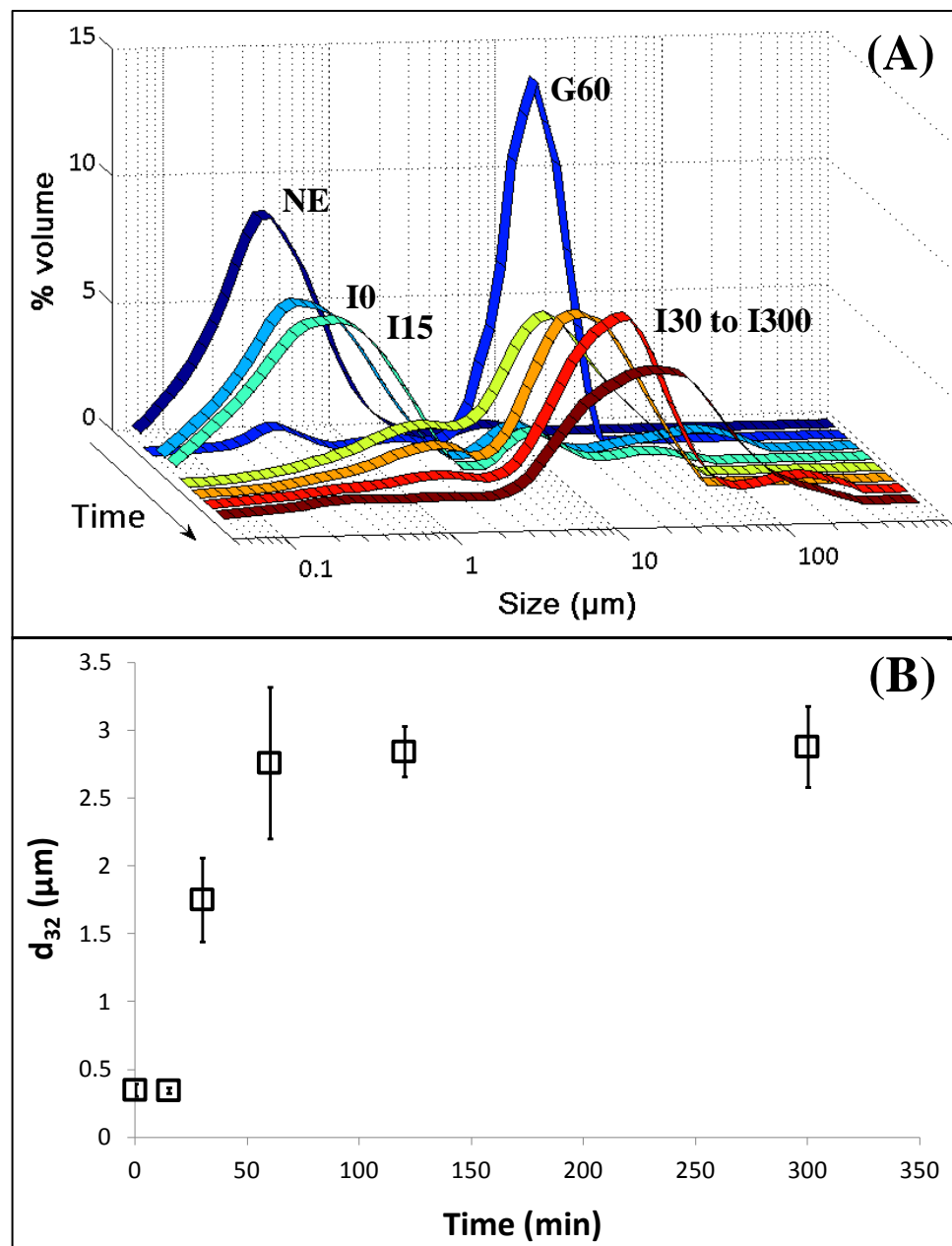


Figure5

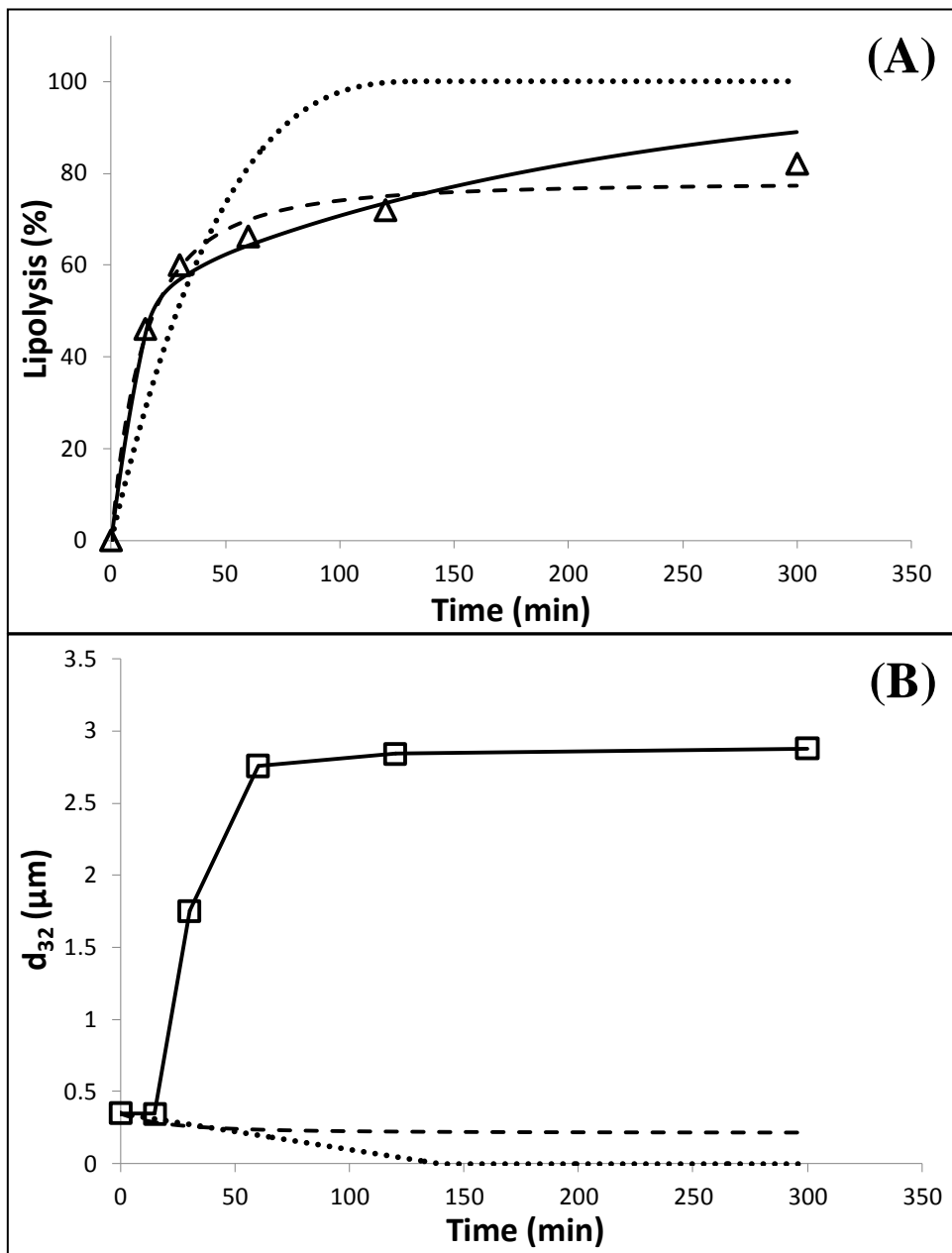


Figure6

